Support Facility for a Mercury-Jet Target Neutrino Factory

September 2001

P. T. Spampinato, J. B. Chesser, D. L. Conner, T. A Gabriel, F. X. Gallmeier, J. R. Haines, T. J. McManamy

Robotics and Process Systems Division

SUPPORT FACILITY FOR A MERCURY-JET TARGET NEUTRINO FACTORY

P. T. Spampinato, J. B. Chesser, D. L. Conner, T. A Gabriel,
F. X. Gallmeier, J. R. Haines, and T. J. McManamy

Date Published: September 2001

CONTENTS

LIST OF FIGURES

LIST OF TABLES

PREFACE

This report summarizes the conceptual design work developed by Oak Ridge National Laboratory for the Target Support Facility of a neutrino-producing research facility. The design is based on using a free-jet mercury target as the source of muons. The Target Support Facility is one of the many systems that make up the overall design of the Neutrino Factory concept developed by the Muon Collider/Neutrino Factory Collaboration. The work presented in this document can be found in Chapter 3 of the final report issued by the Collaboration [1]. This work is based on earlier work for the conceptual design for a target support facility that used a graphite target [2,3].

The basis for much of the design of the Target Support Facility is analytical results of the MARS code, a high-energy physics simulation that establishes hadron yields, magnetic requirements, and shielding estimates. The code simulations were done at Fermi National Accelerator Laboratory [4].

The Target Support Facility consists of the target region where pions and muons are produced, the crane hall that covers the length of the muon decay channel, the hot cell where radioactive components are handled, and various radiation-handling equipment such as manipulators and remotely operated tools. The support facility is a structure approximately 12 m wide by 50 m in length. The unique features of the facility are the free-jet mercury target, the multitude of superconducting solenoid magnets, and the use of water-cooled tungsten-carbide radiation shielding. The report presents details of the various elements of the facility, the design concept for the mercury target system, shielding, remote-handling features of the facility, and a preliminary cost estimate.

ACKNOWLEDGMENTS

ABSTRACT

A conceptual design for a neutrino-producing facility is presented, including the mercury-jet target system, beam absorber, and facility for the target/capture region. The mercury system is a closed loop that includes a containment structure in the high-magnetic field region, a mercury pool beam absorber, conventional equipment such as magnetic-coupled pumps, valves, a heat exchanger, and a special nozzle insert. The superconducting solenoids in the target region are protected from nuclear heating and radiation damage with water-cooled tungsten-carbide shielding; the decay channel solenoids are protected with water-cooled steel shielding. The target region and decay channel have high-neutron fluxes resulting in components that are highly activated. Therefore, the facility configuration is based on remotely maintaining the target system and the magnets, as well as providing sufficient shielding for personnel. Summaries of cost estimates for the target system, magnet shielding, maintenance equipment, and the facility are also presented.

1. TARGET SYSTEM

The Target Support Facility consists of the target region and decay channel, a crane hall over the length of the facility, a maintenance cell at the ground floor elevation for handling magnet components, a hot cell at the tunnel level for mercury target system components, and various remote-handling equipment used for maintenance tasks. The facility is bounded by the proton beam window at the upstream end and the first induction linear accelerator at the downstream end. It contains the equipment for the mercury-jet target, high-field resistive and superconducting solenoids, low-field superconducting solenoids, water-cooled shielding to limit radiation dose and neutron heating to the coils, biological shielding to protect personnel and the environment, and a 50-ton crane that is used for the initial assembly and installation of major components and for subsequent maintenance activities. The target support facility is 12 m wide, and approximately 40 m long. Figure 1 is a view of the overall facility looking downstream from the proton beam line.
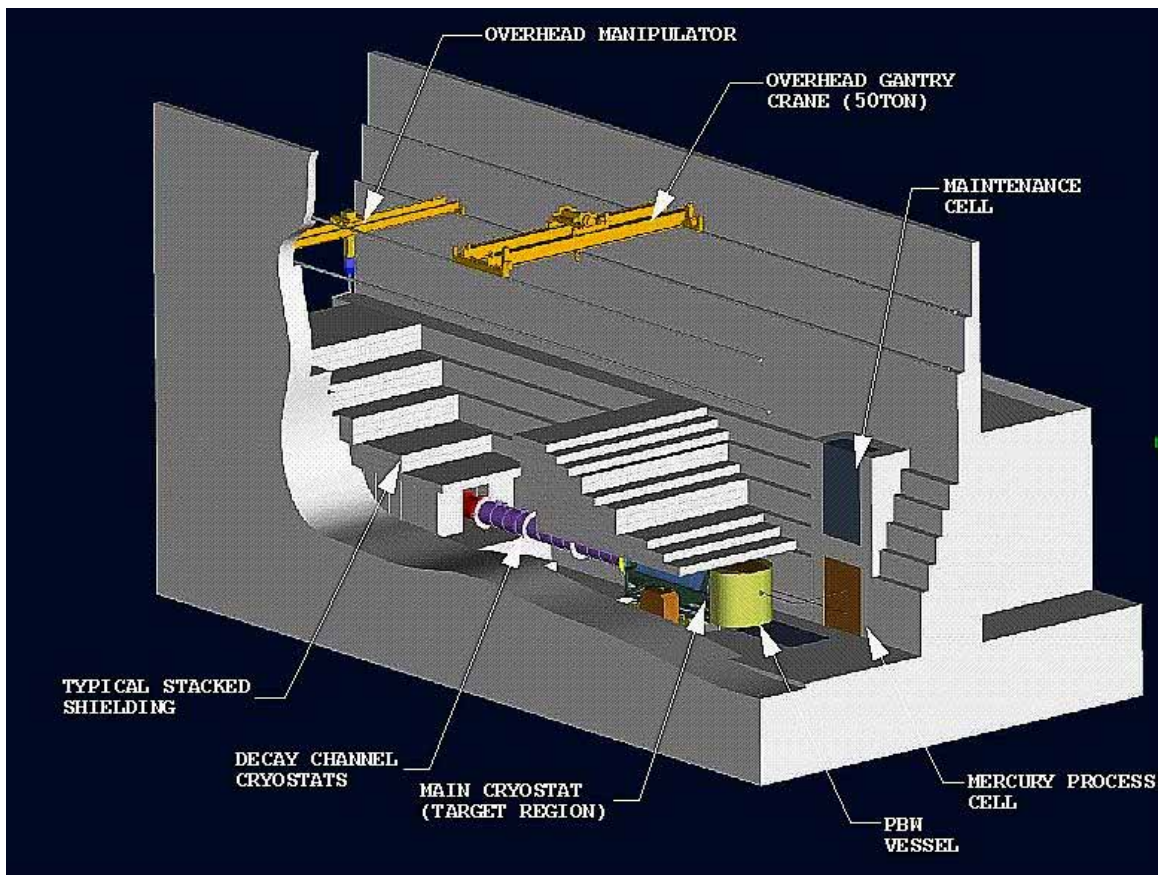
Fig. 1. The overall target support facility.

1.1 TARGET SYSTEM AND PROTON BEAM ABSORBER

The mercury-jet target system consists of the process flow loop, a replaceable nozzle assembly mounted in the bore of the iron plug magnet, a mercury containment vessel that is part of the decay channel downstream to $Z = 6.1$ m, and the beam absorber, which is located at $70 < Z < 245$ cm. A dedicated hot cell that contains the flow loop components is located at the tunnel level. Figure 2 is a schematic diagram of the overall system.
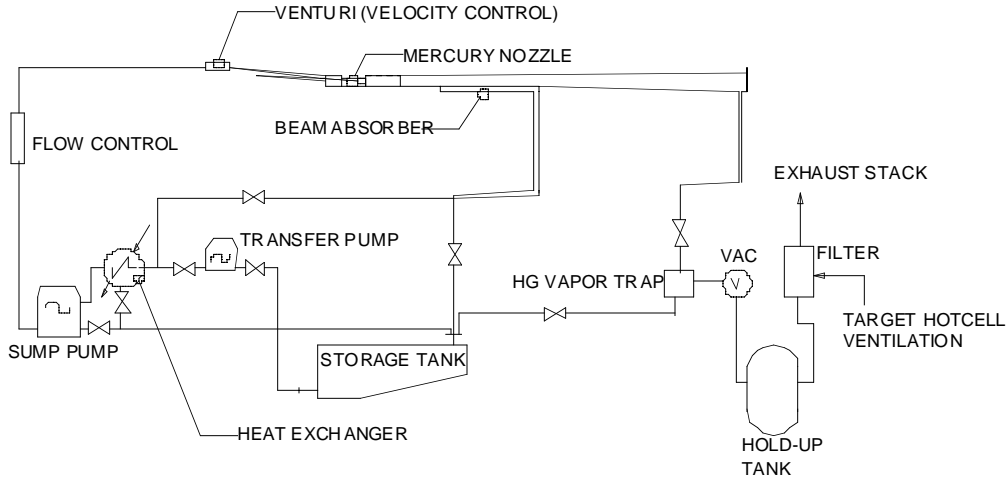
Fig. 2. Target system and beam absorber schematic layout.

The process flow loop contains 110 L of mercury distributed as follows: 30 L in the beam absorber pool, 7 L in the heat exchanger, 35 L in the sump tank, and 38 L in miscellaneous piping and valves. A 200-L tank provides storage for the mercury when the system is shut down or undergoing maintenance. The piping is sloped towards the storage tank, and the elevation of the sump pump, the heat exchanger, the beam absorber pool, and the storage tank are arranged so that the mercury level can be easily controlled among the components. Various valves are used to isolate portions of the system for storage, flow, or drainage into the storage tank; and drainage is by means of gravity. The system components are located in the target hot cell and are arranged to be accessible by the wall-mounted manipulators. The various valves are pneumatically actuated, but they can be manually operated using through-the-wall manipulators, if necessary.

The pumps for the flow loop are centrifugal magnetic drive. The low-capacity pump is self-priming and can pump at a rate of 3–6 gpm. This pump is used to transfer mercury from the storage tank into the flow loop by first filling the heat exchanger and the sump tank of the jet pump. The volume of the sump tank includes the volume of Hg for the absorber pool as well as the jet pump volume (i.e., 65 L). The high-capacity jet pump initially transfers 30 L of mercury into the pool before the high-field magnets are energized. During system operation, it pumps at a rate of 35–50 gpm to circulate mercury at 30 m/s through the nozzle assembly.

The heat exchanger is a welded-tube and shell construction with a closed-loop water system. The inlet temperature of the mercury is 122°C; the outlet temperature is 20ºC. The water inlet temperature is 20ºC; the outlet temperature is 47°C. These results are based on water flowing through the shell of the exchanger at 4 L/s. Figure 3 is a view of the flow loop components located in the target hot cell.

2
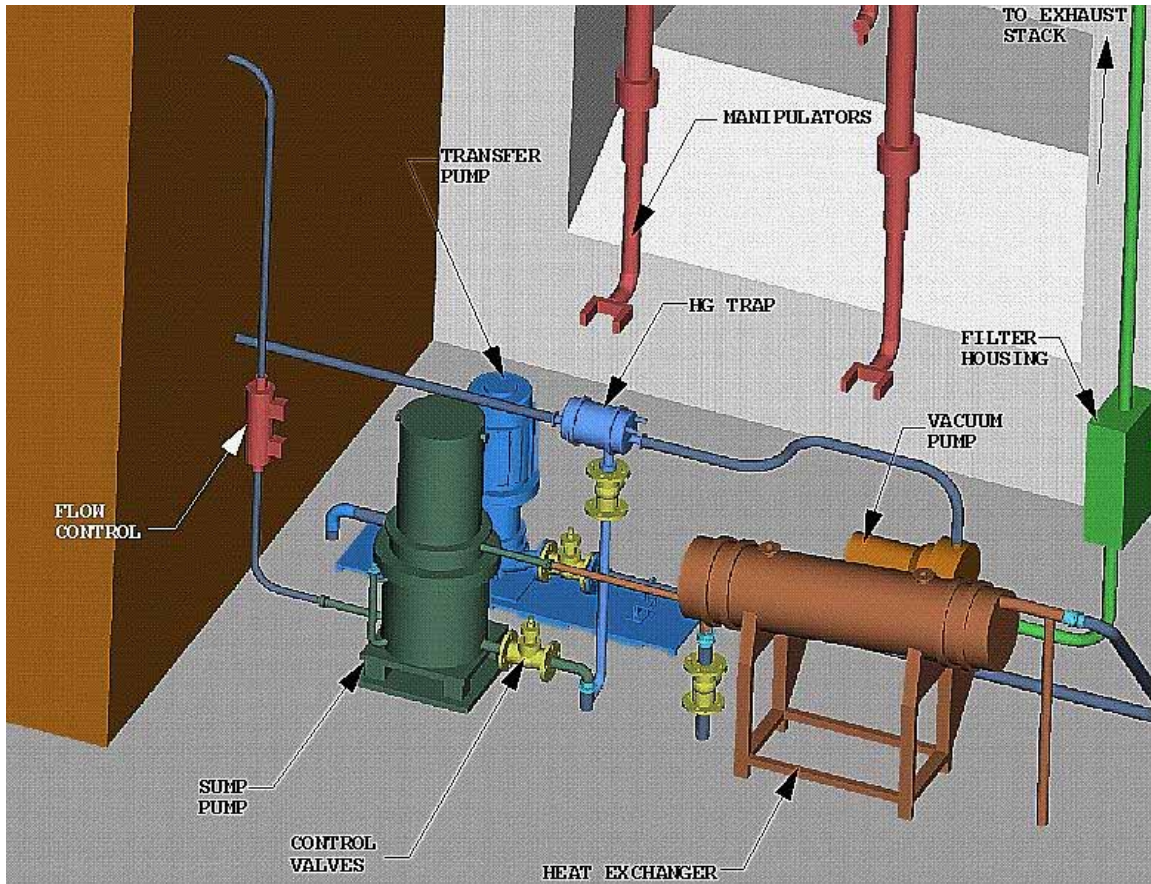
Fig. 3. Arrangement of the mercury flow loop components in the target hot cell.

The mercury storage tank is located under the shield floor in the target hot cell. The full inventory of mercury is stored there when the system is shut down. This storage is accomplished by closing and opening the appropriate valves in the flow loop for gravity flow into the tank. There are drain lines from the sump pump, the heat exchanger, and beam absorber pool. In addition, there is a secondary drain/vent located at Z = 6.0 m. Its purpose is to extract and condense mercury vapors prior to maintenance operations that require opening the mercury containment in the capture/decay region. The vent line is connected in series to a mercury trap (condenser) and a vacuum scroll pump. The condensate is returned to the storage tank by means of a bypass line and the vacuum exhaust passes into the first holdup tank. Gases and mercury vapors are passed through a filter system that contains sulfur-treated charcoal filter modules, before passing into the facility ventilation exhaust.

Mercury, mercury vapors, and rare gas reaction products are contained in the target/capture region by means of windows. The upstream inconel window is mounted on the target nozzle insert at the proton beam line axis; the downstream beryllium window is mounted to the vacuum vessel at SC6. Figure 4 shows the location of the beryllium window.

The average beam power deposited in the jet is 400 W/g (128 kW) and the remainder of the 1 MW proton beam power is assumed to be deposited in the absorber. The bulk temperature rise of mercury in the absorber pool is 102°C, well below the boiling point. However, this assumes homogeneous mixing occurs in the pool caused by the mercury jet that is "injected" into the pool at a rate of 2.4 L/s
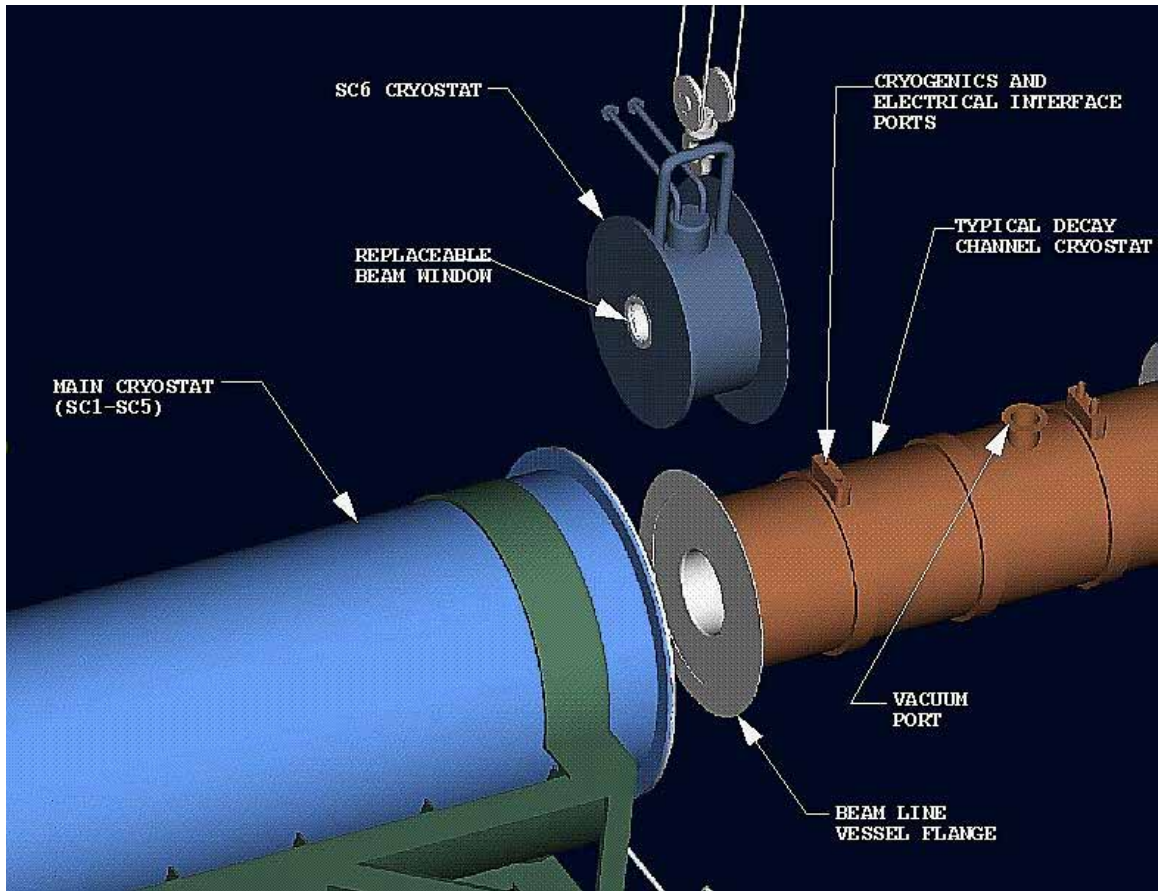
Fig. 4. The beryllium window is mounted to a readily replaceable solenoid.

1.2 TARGET SYSTEM MAINTENANCE

The various components that make up the target system fall into three categories. Class 1 are life-limited components that require frequently scheduled remote replacements during the life of the facility. They are designed for remote handling and minimal impact on operating availability, and remote-handling tools and equipment are included in the cost estimate. Class 2 are lifetime components with activation levels that preclude hands-on replacement, and whose failure shuts down the facility. They have a finite probability of at least one failure. These components are designed for remote handling, but remote-handling tools and equipment are not included in the cost estimate (unless they are used for initial installation). Their replacement could impact operating availability because spare components are not on hand (nor included in the cost estimate). Class 3 components are not expected to fail during the facility lifetime.

Replacement of target system components must be done using remote-handling equipment because of high levels of neutron-induced gamma activation, and the presence of (radioactive) mercury contamination. The target system contains many components that are considered to be life-of-the-facility, numerous components that could require infrequent replacement, and several that are life-limited. The maintenance requirements for this system are summarized in Table 1. The table is based on an operating year of 10^7 seconds, which is the equivalent of 4 months of continuous beam line operation.

4

Table 1. Maintenance requirements for the target system components

Component (Class)	Failure mode	Dose rate (Rad/h)	Expected life (years)	Replacement time (days)[a]
Nozzle Insert (1)	Erosion, embrittled beam window	$>10^6$	2–3	11–16
Beryllium Window (1)	Embrittlement	10^4–10^5	2	7–11
Isolation Valve (1)	Mechanical	10^4–10^5	5–7	1–2 (plus time for beryllium window repl.)
Filters (1)	Saturated	Contam.	2	2–3
Pumps, Valves (2)	Mechanical	Contam.	7.5	2–3
Heat Exchanger, Piping, Tanks (3)	Mechanical	Contam.	>40	5–8

[a]Based on assuming either 12-hour or 8-hour maintenance shifts.

1.3 TARGET SYSTEM COST

The costs associated with the mercury-jet target system are listed in Table 2. These estimates include the cost of materials, engineering design, fabrication, installation, and a percent-based cost for quality assurance, inspection, and procurement. The costs do not include research and development (R&D), overhead burdens, or contingency.

Table 2. Summary of target system costs

WBS Item No.	Subsystem Name	Cost ($K)
1.2.3	Mercury jet system	
1.2.3.1	Storage tanks	51.6
	1—200-L Hg storage tank, 1—70-L sump tank, 3—1950-L gas hold up tanks	
1.2.3.2	Pumps	55.0
	1—magnetic drive transfer pump, 1—magnetic drive sump pump, 1—vacuum scroll pump	
1.2.3.3	Piping	21.1
	1 in. and 1-1/2 in. sch. 40 stainless piping, flanges, …	
1.2.3.4	Nozzle and valves	68.8
	Nozzle insert + 1 spare insert; inconel beam window, 1 in. and 1-1/2 in. actuated valves, flow control valve, …	
1.2.3.5	Downstream collection/containment	284.1
	Steel vessel insert ($-45 < Z < 610$ cm), 330-mm isolation valve, 330-mm beryllium window, mercury vapor condenser, air exhaust filter	
1.2.3.6	Heat exchanger (1.2^6 Btu/h)	32.8
1.3.2	Beam absorber costs are included in 1.2.3	
	Total cost	513.4

1.4 TARGET SYSTEM DESIGN ISSUES AND NEAR TERM R&D

Two major assumptions for the target system design were made for this pre-conceptual design study. The first assumption is that heating of mercury in the beam absorber pool is nearly uniform and any localized heating does not exceed the boiling temperature. The second assumption is that the mercury-jet emerges from the target interaction region as a stream and contributes to the thermal mixing in the pool. Additional simulations need to be carried out to better understand these suppositions, and tests with a mercury-jet in an appropriate magnetic field are needed to study the downstream effects on the jet. Two near-term R&D activities are recommended to address these, as well as testing to assess the lifetime of the nozzle.

1. Determine the state of the mercury-jet downstream from $Z = 0$ to assess whether an active mixing system is needed in the absorber pool. Develop design concept as required.
2. Quantify the extent of erosion of the mercury-jet nozzle and determine the impact to nozzle lifetime. Test various materials at jet velocities up to 50 m/s; an obvious material choice for a 1-cm diameter insert is tungsten.

2. TARGET SUPPORT FACILITY

The geometry for the target support facility is defined around the intersection of the mercury jet, the proton beam, and the magnetic axis of the solenoid magnets. The proton beam interacts with the jet over a 30-cm region so that the downstream interaction point is at $Z = 0$ cm, and the upstream interaction point is at $Z = -30$ cm. The three axes intersect at $Z = -15$ cm. The location of the coils and other components is measured from $Z = 0$. The decay channel extends to $Z = 35.60$ m, which is the facility interface with the first induction linear accelerator. Figures 5 and 6 show the basic geometry of the facility and its boundaries.

The proton beam window is located at $Z = -330$ cm and is connected to the core vacuum vessel with a removable section of beam pipe. This design permits the window assembly to be close to the target region, yet readily removable to replace the window or the mercury jet nozzle or to provide clearance for the replacement of the inner solenoid module should that ever become necessary (Fig. 15).

It is important to keep in mind that virtually all of the components that make up the target and capture facility will be highly radioactive; therefore, replacing components after start-up operations must be done using remote-handling equipment and tools. The development of the facility arrangement was
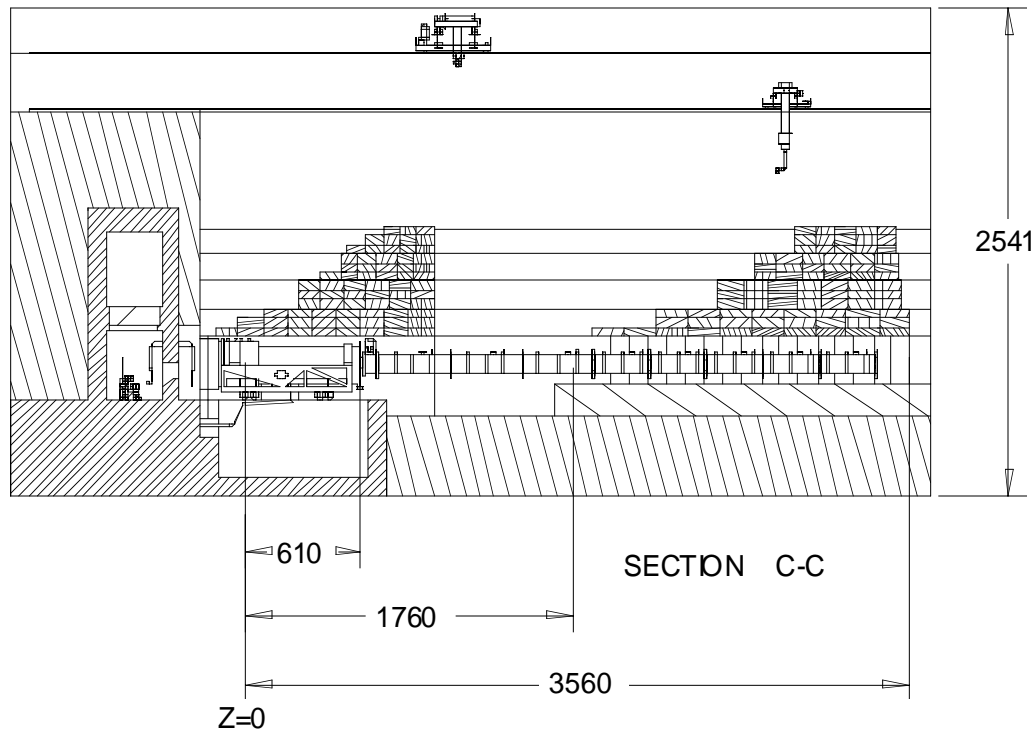
Fig. 5. Slide elevation of the facility geometry.
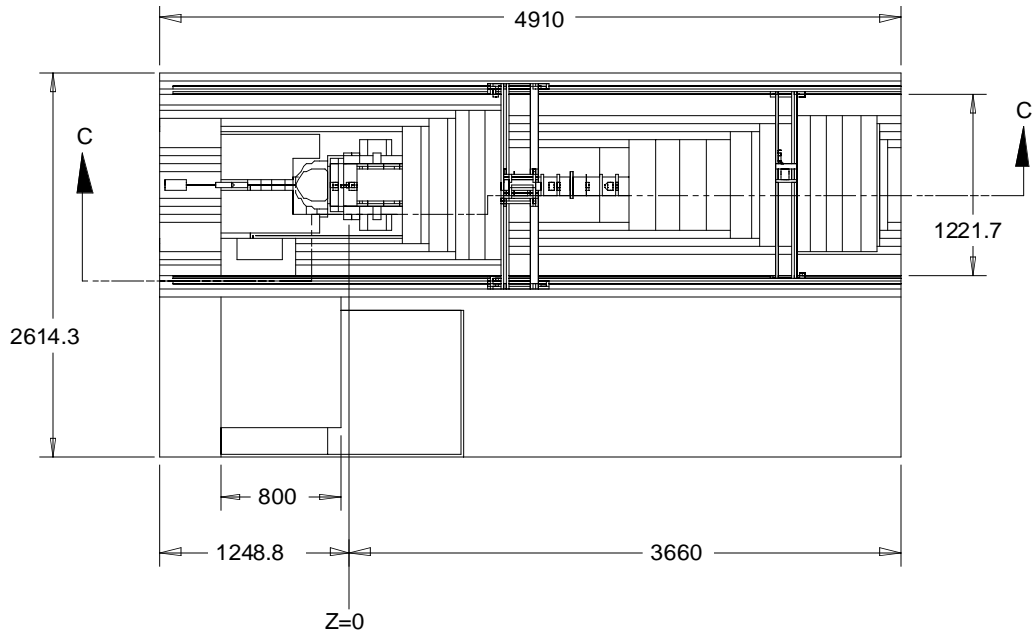
Fig. 6. Plan view of the facility geometry.

based on considering the initial assembly and installation of the various subsystems and also on modularization of components to simplify remote handling and have minimal impact on the operating availability.

2.1 SOLENOID MAGNETS

The solenoid magnets are located in the capture and decay tunnel of the support facility, and although they are considered to be lifetime components, the facility design is based on their remote replacement. The tunnel begins in the target region upstream of the proton beam window and extends to Z = 35.6 m. The first five solenoids (SC1–5) are contained in a common cryostat that extends to Z = 6.1 m. The cryostat is designed so that its inner shell is the outer shell of part of the tungsten-carbide shield. Therefore, there is a shield cylinder attached to the cryostat that is 16–20 cm thick and contains inner rib supports to stiffen this cylindrical beam. The ribs are also partitions for the cooling flow channels of the shield. Figure 7 is a section through the main cryostat that shows the magnet arrangement and the shield beam. Figure 8 shows the rib structure of a typical shield module and the coolant line connections.

There is a separate module for the resistive magnets and shielding contained within the bore of SC1. It consists of an iron plug, three resistive, water-cooled magnets (HC1–3), and tungsten-carbide shielding. The combination of these coils and SC1 provide the 20 Telsa field-on-axis in the target region. Figure 9 shows the resistive coil module along with the nozzle insert for the mercury jet. Figure 10 shows a section cut and end view of the resistive module. The target nozzle insert is mounted in the off-center cutout in the iron plug.
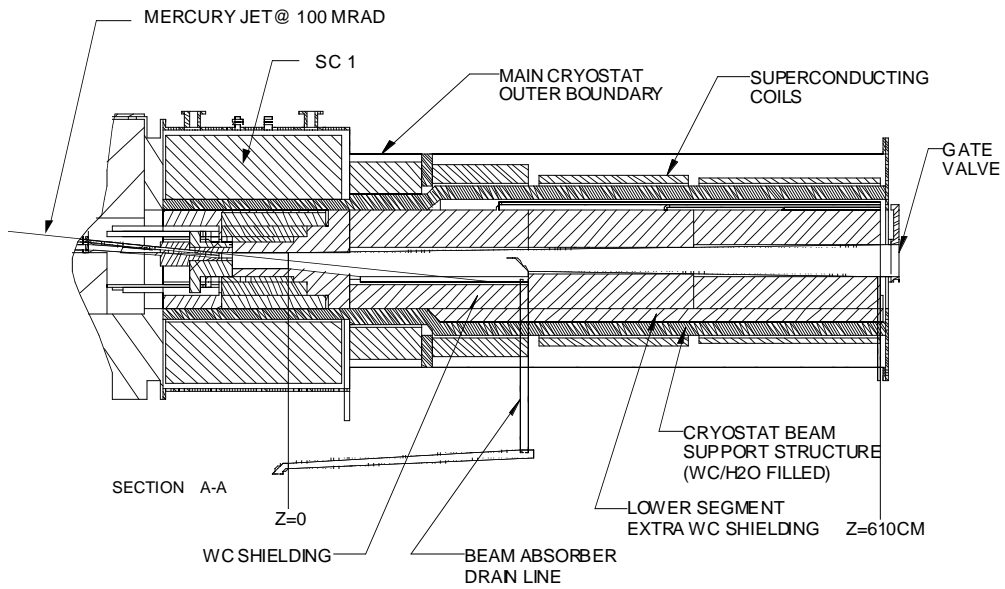
Fig. 7. Main cryostat containment for SC1–5.
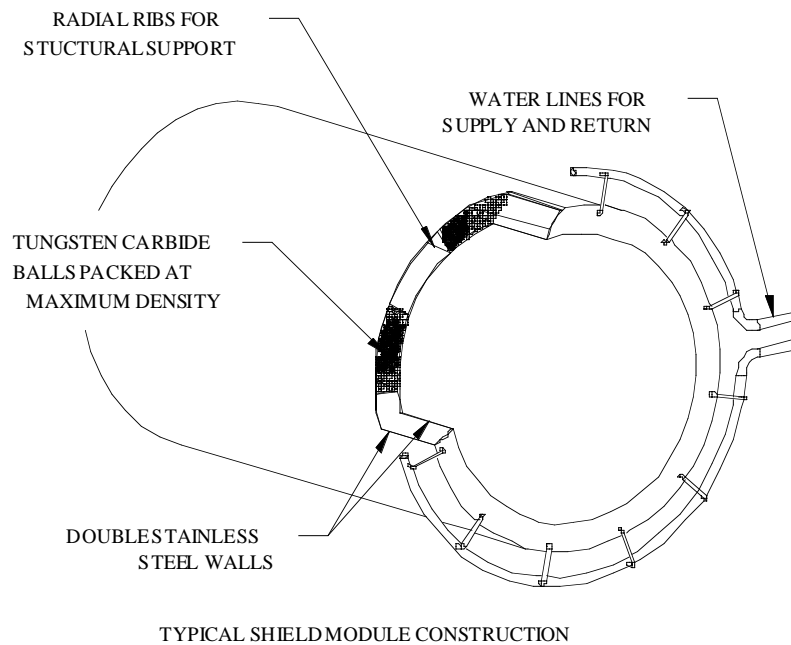
Fig. 8. Typical construction for the shield modules.
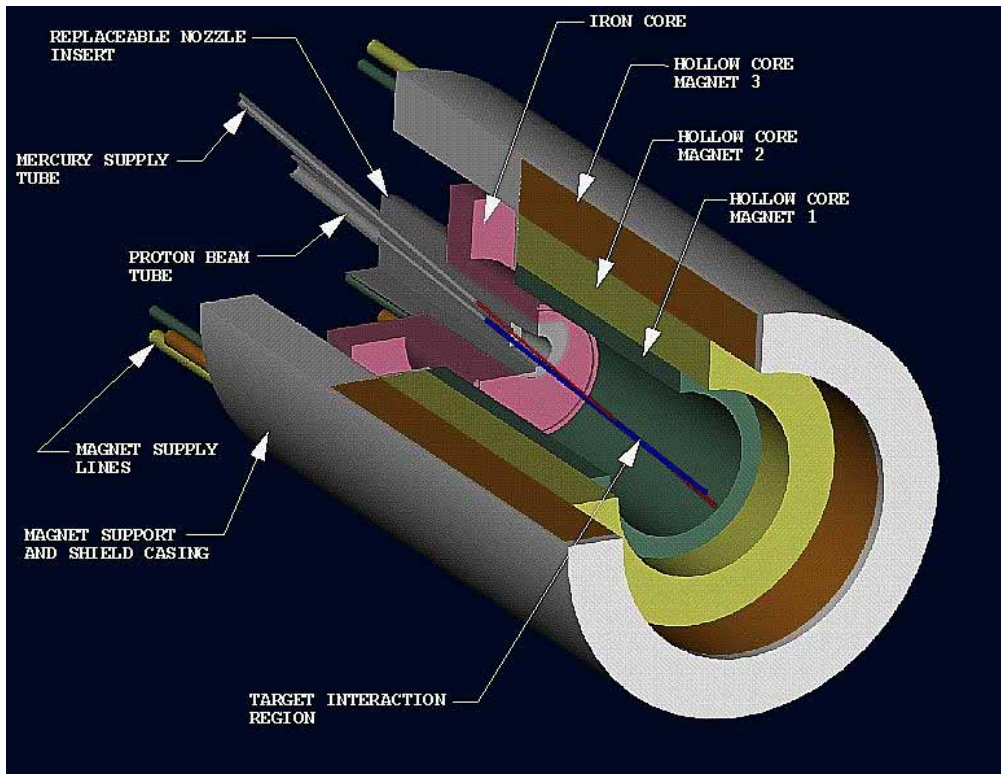
Fig. 9. The resistive coils/shield module.
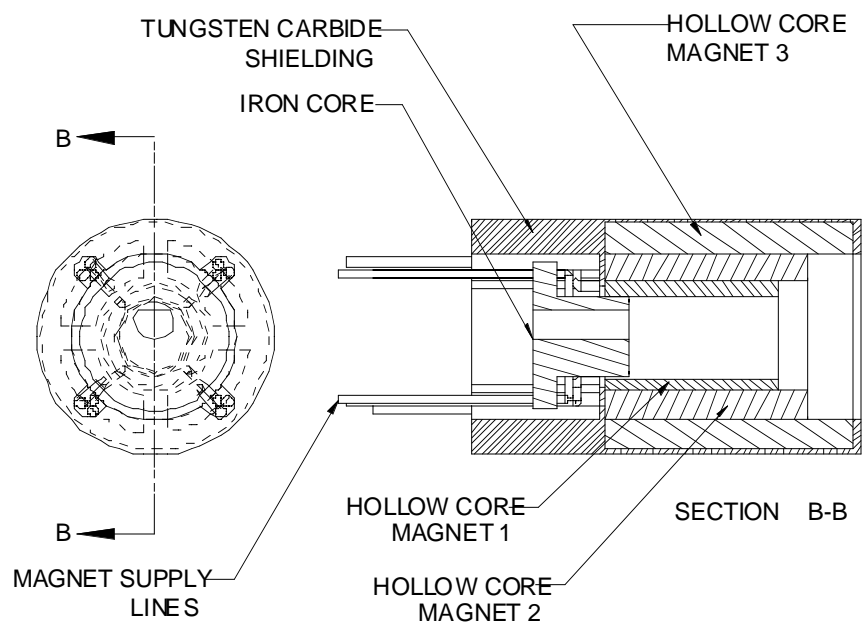
Fig. 10. Section cut and end view of the resistive coil module.

10

The magnets downstream of the main cryostat are two-coil solenoids contained in 4-m long cryostats, except for SC6, which has a 0.5 m cryostat. These extend from Z = 6.1–17.6 m and make up the remainder of the transition coils (SC6–12). Figures 1 and 4 show the transition coils. In this region, the field-on-axis decreases until it is 1.25 T at Z = 17.6 m.

Coil SC6 is smaller and is designed to be the mounting support for the beryllium window located at Z = 6.1 m. The window is the downstream containment boundary for the mercury target vessel. The window is replaced every 2 years by removing SC6 and installing a spare SC6 module with the replacement window already mounted. Figure 4 shows SC6 in the process of being removed.

The magnets from the end of the transition region to the end of the decay channel are contained in 3-m long cryostats, each containing three coil-pairs. Figure 11 is a section- and end-view of a typical cryostat module. The nuclear shielding for these magnets is similar to the upstream coils except that a homogeneous mix of steel balls is used instead of the tungsten-carbide balls.
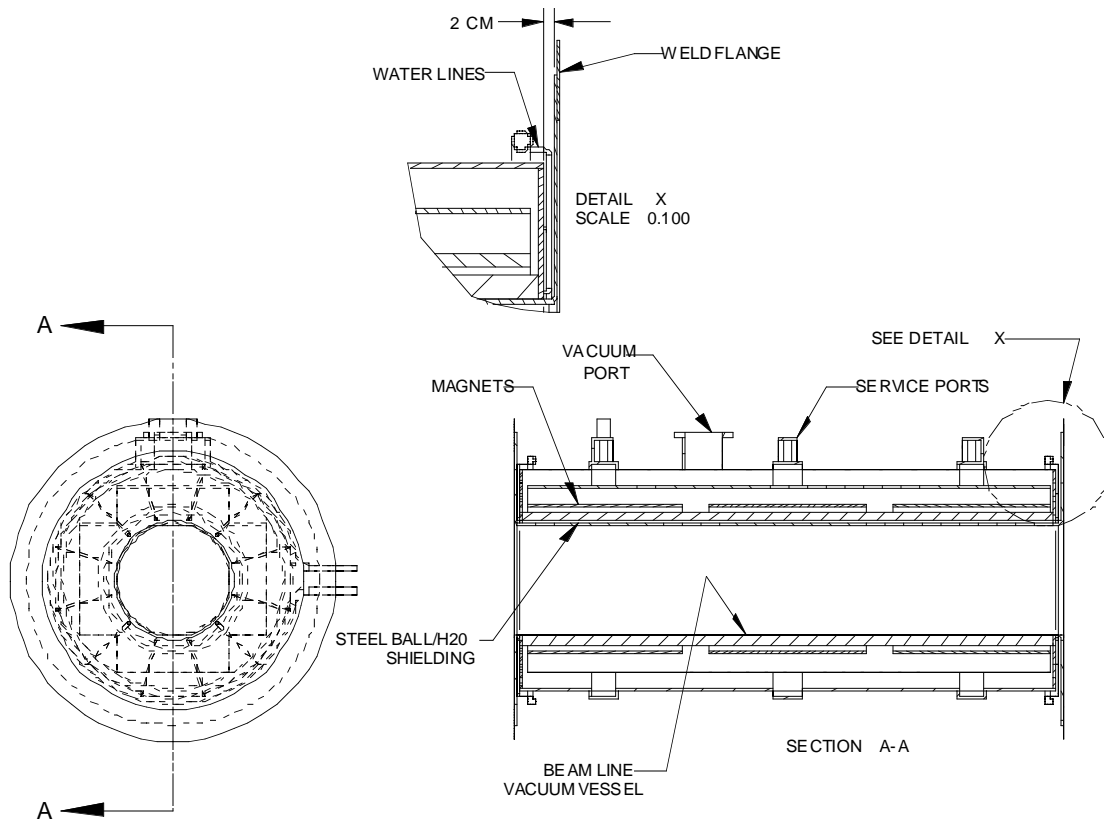
Fig. 11. Decay channel cryostat module.

11

2.2 ASSEMBLY AND INSTALLATION

The assembly and installation of the magnet system was the major consideration for determining the facility arrangement. The coil/shield modules are the heaviest and largest components and were the basis for establishing the building height and width, and determining the crane capacity needed for installation operations and subsequent maintenance.

The overall dimensions of the coil modules and their respective component weights are given in Table 3. The largest module weight was used to determine the lifting requirement in the crane hall. Installing the tungsten-carbide shield for SC4–5 is the heaviest lift at approximately 43 tons. A 50-ton bridge crane with a 46-ft span was chosen.

Table 3. Solenoid coil sizes and weights, and shield module weights

Component	Outer diam. (cm)	Length (cm)	Module wt (lb)
Resistive module	110	180	47,500
Iron plug	–	–	–
HC1	–	–	–
HC2	–	–	–
HC3	–	–	–
W-C shield	–	–	–
Main cryostat + shield beam	270	740	73,600
SC1	256	178	61,000
SC2–3	202	183	21,700
2–3 shield	128	183	59,600
SC4–5	176	351	17,900
4–5 shield	148	351	86,400
SC6 + shield	104	50	<4,000
SC7 + shield	104	185	11,800
SC8 + shield	104	185	10,800
SC9 + shield	104	185	9,600
SC10 + shield	104	185	8,400
SC11 + shield	104	185	7,700
SC12 + shield	104	185	6,600
Decay coils + shield (6)	87	296	12,600

2.3 HIGH-FIELD REGION

The high-field coils provide a 20-Tesla field in the target region and consist of three resistive coils (HC1–3) and an iron plug surrounded by a water-cooled tungsten-carbide shield (Figs. 9–10), and an outer superconducting coil (SC1, Fig. 7). The HC coils and part of the shield constitute a single module that is installed into the cryostat of the high-field superconducting coil.

2.4 COIL-TO-COIL FORCES/METHOD OF SUPPORT/METHOD OF ASSEMBLY

The net force between SC1–12 is nearly zero, meaning it is a balanced system. SC1 reacts to the forces of SC2–12 with an equal and opposite force. However, the coil-to-coil forces between individual magnets are large. SC1 reacts to the accumulated forces of the downstream coils with 23 million pounds (102.5 kN). The forces from SC2–5 are, respectively, 10.3E6 lb, 6.6E6 lb, 3.4E6 lb, and 2.3E6 lb. (The force contributions from SC6–12 are ignored here because they are small by comparison).

To minimize heat leaks into the SC1–5 cryostat caused by large-area cold-to-warm-to-cold supports, use of a common cryostat was chosen by the solenoid coil designers. Therefore, the coil-to-coil supports are cold, but the cryostat structure must support the total gravity load of coils SC1–5. This is accomplished by making a cylindrical portion of the radiation shield part of the cryostat (Fig. 7).

2.5 TRANSITION FIELD COILS

The cryostat is assembled from two sections onto a continuous cylindrical beam that is part of the radiation shield. The cryostat/beam assembly is lowered into the target region of the tunnel, onto a pair of trunnion supports. The trunnion is located midway along the cryostat to minimize the depth of pit area under SC1–5, and to minimize the elevation of the crane for installing SC4–5. The cryostat is rotated so that the upstream end points up for the installation of SC1. The weight of the SC1 is 61,000 lb. The bridge crane is used to assist lowering the main cryostat so that the downstream end points up and the coil module consisting of SC2–3 is installed followed by its inner shield. The cryostat is then rotated again with assistance from the crane so that the upstream end points up. The resistive coil module (iron plug, HC1–3, and shielding) is then installed into the inner bore of the shield-beam. The cryostat position is reversed again and module SC4–5 is installed followed by its inner shield. This sequence is necessary for initial installation to stay within the 50-ton load limit of the crane. Figure 12 shows the installation sequence of the coils that are installed into the main cryostat.
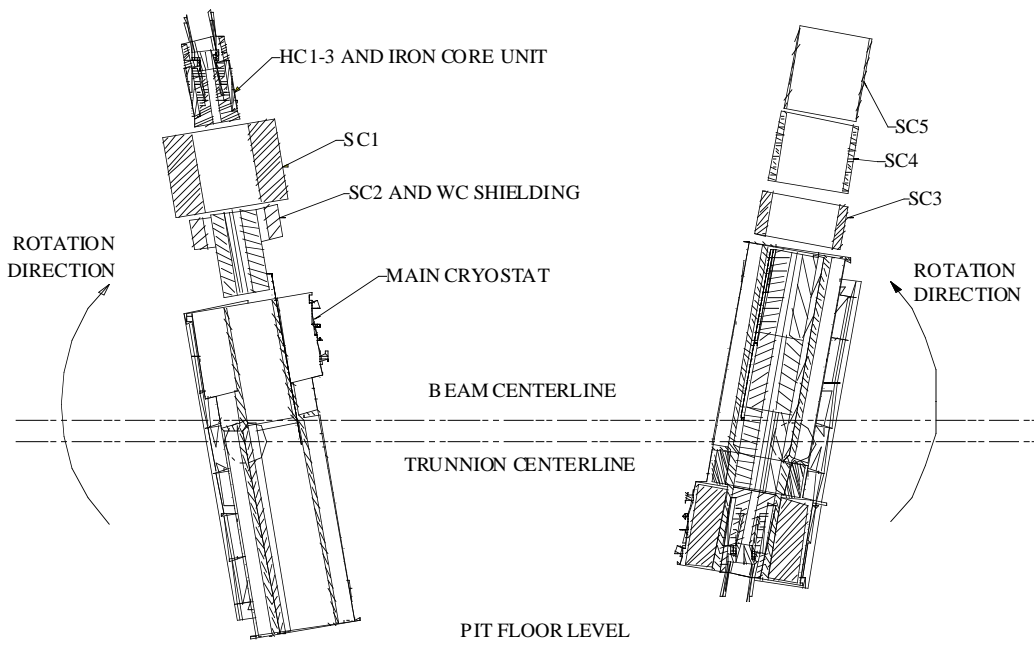
Fig. 12. Installation sequence for the high-field coils SC1 and HC1–3, and transition coils SC4–5.

2.6 DECAY CHANNEL COILS

Each of the remaining cryostat modules contains a 5-cm thick radiation shield beam mounted to the inner diameter of the cryostat shell. For the coils downstream of Z = 610 cm, the shield material is water-cooled copper or stainless steel. A homogeneous mix of stainless steel balls (2 < d < 6 mm) is judged to be the most cost-effective approach, and was used for the design and the cost estimate.

A separate vacuum boundary for the muon decay channel is pre-installed to the inner shell of each shield/cryostat assembly. These are assembled so that the outer flange of the vacuum boundary shell can be seal-welded to the flange of adjacent modules, and subsequently cut for disassembly. Figure 11 shows the typical side view and end view of the decay channel magnets, the vacuum flange attachments, and clearance for coolant lines.

2.7 COIL REPLACEMENT AND REMOTE HANDLING

The solenoid magnets are designed to be lifetime components. However, they are configured for remote replacement in the event of failure since they will become highly activated and since the ability to replace any of them is critical to the operation of the facility. The reverse of the assembly procedure described above is the disassembly method to replace any of the coils. Removal of any solenoid cryostat requires removing at least 24 shield slabs covering the tunnel. Each shield piece weighs 45 tons, and there is ample space on the crane hall floor to stack the shielding. When the process of removing shielding is started, personnel access to the crane hall is not permitted, and removal operations must be done remotely using the bridge-mounted manipulator system. The maintenance cell located above the target hot cell is configured to accommodate the cryostat modules for subsequent dismantling and waste disposal. The maintenance cell is located adjacent to the staging area where new components are delivered and where waste disposal casks are shipped out of the facility. Figure 13 shows the maintenance cell and its relation to the target region and the staging area.

2.8 FACILITY SHIELDING

The facility shielding is designed to permit unlimited access for radiation workers in the crane hall. The shield material and thickness limit the dose rate at the crane hall floor to 0.25 mrem/h (0.0025 mSv). A Monte Carlo neutron, photon, charged particle transport code (MCNPX) using cylindrical geometry was prepared for neutronic calculations. The results show that the shield over the target region should be 5.8-m thick and the shield over the decay channel should be 5.2 m thick. For the purpose of this design, an average thickness was used throughout consisting of 5.2 m of steel to attenuate fast neutrons and 0.3 m of concrete to attenuate slow neutrons. The model analyzed the shielding requirement downstream to Z = 3600 cm, but it is clear that beyond the decay channel, into the first induction linear accelerator and beyond, similar facility shielding is needed, and the solenoid components will have dose rates too high to permit hands-on maintenance. Therefore, the crane hall and the remote handling access that it provides to the target/capture magnets should extend well beyond the end of the decay channel. It may be assumed that the same crane hall configuration could be used to service the linear accelerator regions downstream, several hundred meters to the storage ring.

Figure 14 is a typical cross section in the decay channel showing the arrangement of removable shield slabs. The dimensions for each shield piece are determined by limiting their weight to 45 tons. The amount of shielding needed to limit the dose rate in the crane hall to 0.25 mrem/h is 5.2 m of steel, covered with a 30-cm concrete layer. Each slab layer is 46-cm thick, but the length and width varies, so each layer has offset joints that avoid a streaming path to the crane hall. It should be noted that the width of the tunnel decreases from 7 m in the target region to 5.2 m at approximately Z = 700 cm because of the smaller diameter of the magnets downstream from SC7.

The shield requirement upstream of the target region to attenuate backscattering is 2.6 m of steel. This thickness was chosen to limit dose rate to 1 rem/h. A stacked assembly of steel blocks is

located in the 3-m diameter vacuum vessel that encloses the proton beam window and the mercury-jet nozzle. The beam window is located at $Z = -330$ cm and is attached to the beam pipe feedthrough with a Grayloc® or Reflange® remote connector. (The beam pipe diameter is assumed to be 25 cm although that is not a limiting factor for the remote connector.) This type of connector is well suited for reliable, robust operations that are done frequently. Figure 15 is a section view of the vessel showing the arrangement of the components it contains and the relation with the target system. Removal of the nozzle insert and resistive coil module is through the vacuum vessel after removing shield segments.
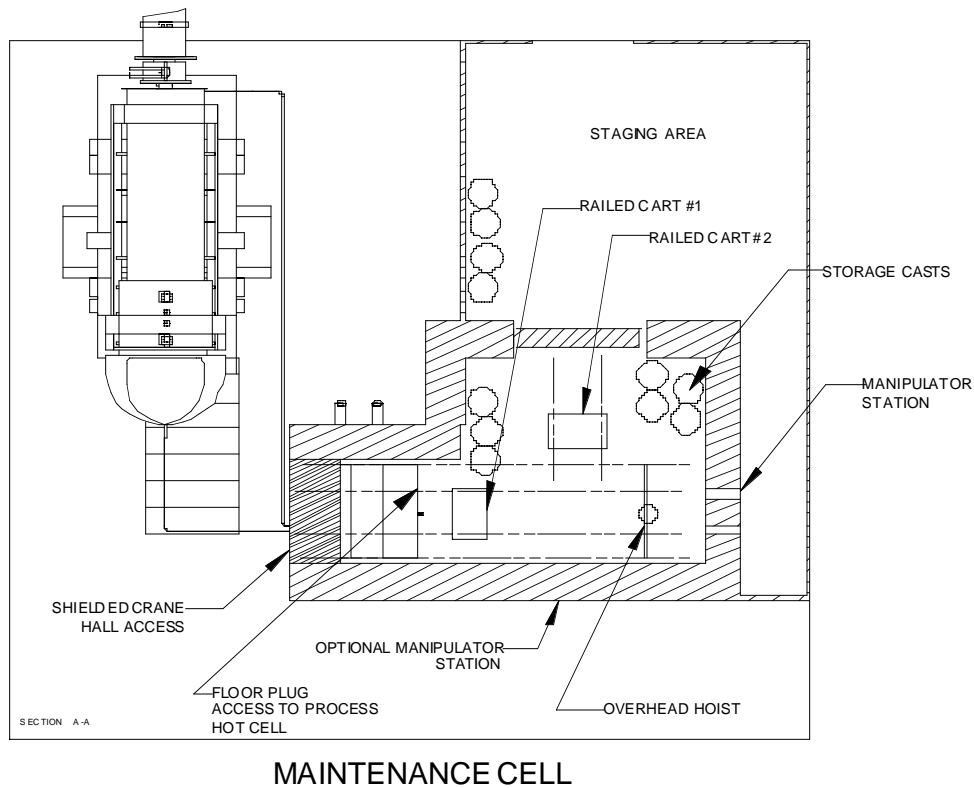
Fig. 13. The maintenance cell.

2.9 MAINTENANCE OPERATIONS

The components in the target/capture facility fall into three categories. Class 1 are life-limited components that require scheduled remote replacements during the life of the facility. They are designed for remote handling and minimal impact on operating availability, and remote-handling tools and equipment are included in the cost estimate. Class 2 are lifetime components with activation levels that preclude hands-on replacement, and whose failure shuts down the facility. They have a finite probability of at least one failure. They are designed for remote handling, but remote-handling tools and equipment are not included in the cost estimate (unless they are used during initial installation). Their replacement will impact operating availability since spare components are not available. Class 3 components are not expected to fail during the facility lifetime. The basic maintenance requirements for the facility are summarized in Table 4.

SECTION B-B
DECAY CHANNEL SHIELDING
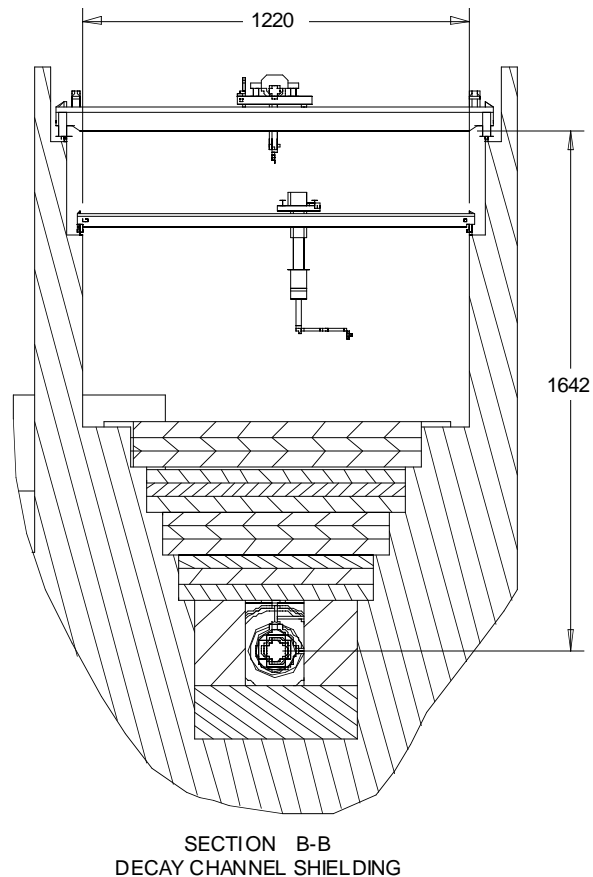
Fig. 14. Facility shield over the decay channel.

16

2.10 COST

The costs associated with the target/capture facility, including nuclear shielding for the target and capture solenoids, are listed below. These estimates include the cost of materials, engineering design, fabrication, installation, and a percent-based cost for quality assurance, inspection, and procurement. The costs do not include R&D, overhead burdens, or contingency. Table 5 summarizes the solenoid shield costs, and Table 6 summarizes the facility costs.

Several issues are related to the facility configuration and design of the nuclear shielding for the solenoids. The first facility issue deals with the location and access of the target and magnet support
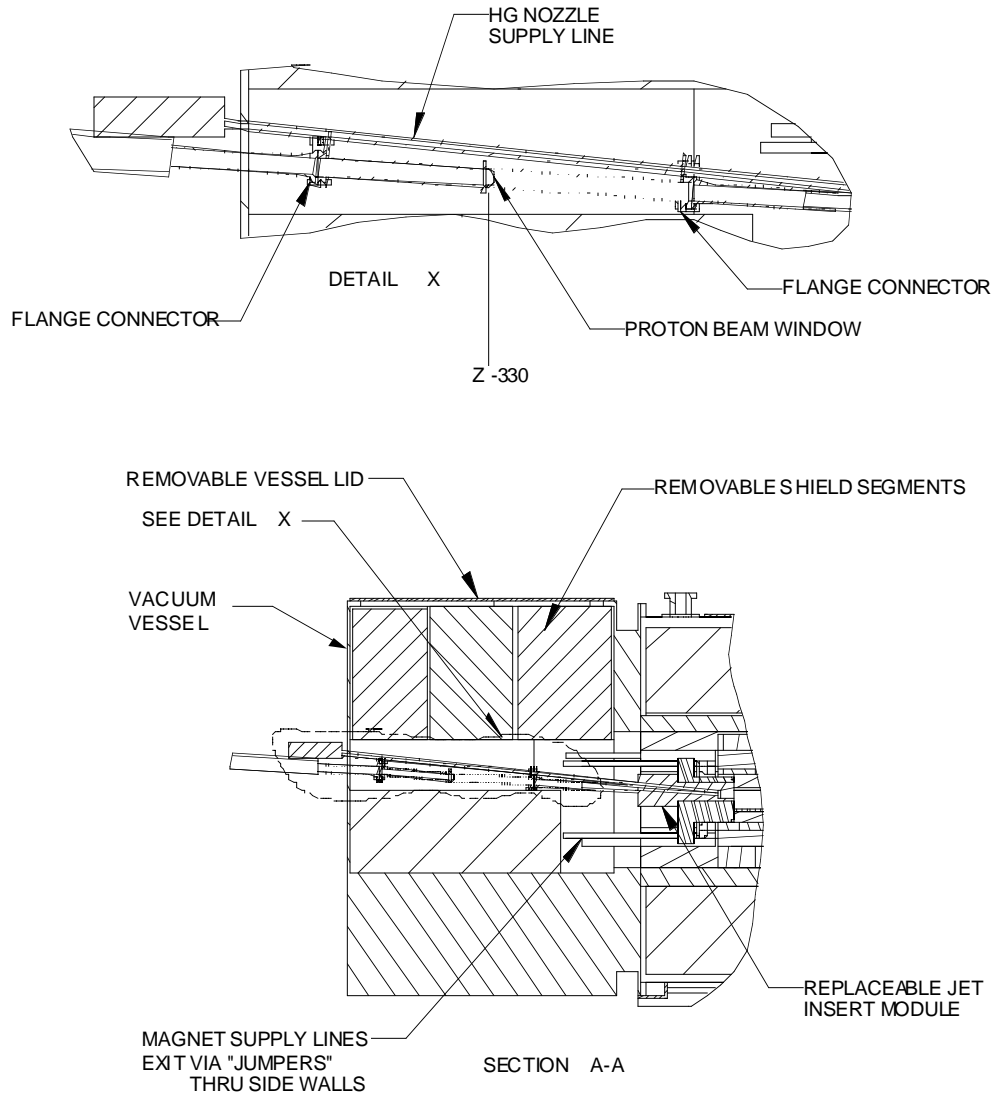
Fig. 15. Vacuum vessel upstream of the target region.

Table 4. Maintenance requirements for the target/capture components

Component	Expected life (years)	Replacement time (weeks)
Proton beam window	2	1
Vacuum pumps, valves, …	7	1–2
Resistive solenoid module	>40	30–40 (includes time to fabricate a replacement)
High-field solenoids	>40	50–60 (includes time to fabricate a replacement)
Transition-field solenoids	>40	30–40 (includes time to fabricate a replacement)
Low-field solenoids	>40	20–30 (includes time to fabricate a replacement)

Table 5. Summary of solenoid shield costs

Nuclear Shield (high-field and transition solenoids)	$K
Tungsten-carbide shield + shield structure for SC1–6 (includes one spare SC6)	9,312.3
Steel shield + structure for SC7–12	674.5
Solenoid magnets	
Nuclear shield (steel shield + structure for low-field solenoids, $17.6 < Z < 35.6$ m)	278.5
Shield cost	10,265.3

Table 6. Summary of facility construction costs

Target and capture facility	$K
Crane hall/tunnel	4,642.5
Steel shield slabs	8,589.8
Hot cell (target system)	109.8
Maintenance cell	260.7
Maintenance equipment	1,680.5
Engineering design, QA&I, procurement	3,240.1
Facility cost	18,523.4

systems, namely, vacuum pumps, ducts, and valves; cryogenic and electrical lines routing; and diagnostic equipment, as examples, to ensure that they are readily maintainable. A target hot cell is already configured with access and maintenance in mind, and a more detailed iteration of the facility design would accomplish the same for the other support systems. The second facility issue is the extent that remote-handling capability and equipment are needed downstream from the target/capture region. An extrapolation of the shield analysis that was done for the floor shield over the tunnel, $-80 < Z < 3600$ cm, indicates that similar requirements apply downstream. This requirement will have an impact on the overall facility cost.

2.11 FACILITY DESIGN ISSUES AND NEAR-TERM R&D

Several issues that deal with the nuclear shield design could be addressed with R&D activities that simultaneously address mechanical and thermal questions. It has been determined that the optimum shield for the high-field solenoids is 80% tungsten-carbide and 20% water, and the shield design is based on using tungsten-carbide balls. Scale-model tests are needed to investigate how to distribute the balls in a homogeneous matrix, and to assess properties such as pressure drop and heat-transfer

coefficient, to name two. This shield is a costly component, and it is important for it to be efficiently designed.

3. CONCLUSIONS

The conceptual design of a target support facility was developed for a neutrino-producing research facility. The design is based on using a free-jet mercury target that interacts with a 24-GeV, 1.5-MW proton beam. The mercury volume is 110 L, and is recirculated in a closed-loop confinement system. The target is located in a high-field (20 T) solenoid magnet region consisting of three resistive coils, an iron core, and a Nb3Sn superconducting coil. Muons are collected in the decay channel, which consists of low-field (1.25 T) solenoid, NbTi superconducting magnets. Because of high-neutron fluxes produced in the target region, use of remotely operated equipment is required to maintain the target system, including the decay channel. A preliminary cost estimate was prepared in support of the design effort. The level of preconceptual design work presented in this report demonstrates the feasibility of developing this concept in a cost-effective manner. Additional design details should be developed for the mercury target system, based on the results of R&D testing that target stability in high-magnetic fields. In addition, further design details should be developed for the various utility connections that the target system and the magnets require to fully quantify remote-handling issues and needs.

4. REFERENCES

1. S. Ozaki, R. B. Palmer, M. S. Zisman, C. Gallardo (editors), "Feasibility Study-II for a Muon-Based Neutrino Source, June 14,2001, http://www.cap.bnl.gov/mumu/studyii/final_draft/The-Report.pdf.
2. N. Holtkamp et al., "FNAL Feasibility Study on a Neutrino Source Based on a Muon Storage Ring," Fermi National Laboratory, Batavia, Illinois, April 2000, http://fnal.gov/projects/muon_collider/ nu-factory/.
3. P. T. Spampinato, et al, *Support Facility for a Graphite Target Neutrino Factory*, ORNL/TM-2000/153, Oak Ridge National Laboratory, Oak Ridge, Tennessee, August 2000.
4. N. Mokhov, Particle Yield and Radiation fields in Feasibility Study-2 Target Capture System, MUC0194, March 21, 2001, http://www-mucool.fnal.gov/mcnotes/muc0194.txt

.

INTERNAL DISTRIBUTION

1. F. E. Bertrand
2. T. W. Burgess
3. J. B. Chesser
4. D. L. Conner
5. P. Ferguson
6. T. A. Gabriel
7. F. X. Gallmeier
8. R. G. Gilliland
9. J. R. Haines
10. J. N. Herndon
11. N. Holtkamp

12. R. A. Lillie
13. T. E. Mason
14. T. J. McManamy
15. G. E. Michaels
16. F. G. Pin
17. S. L. Schrock
18-22. P. T. Spampinato
23. C. N. Strawbridge
24. ORNL Central Research Library
25. Laboratory Records

EXTERNAL DISTRIBUTION

26. Sam Childress, Fermilab, P.O. Box 500, BD-NUMI, Mail Station 220, WH 12W, Batavia, IL 60510-0500
27. David Finley, Fermilab, P.O. Box 500, TD–Administration, Mail Station 316, ICB 2W, Batavia, IL 60510-0500
28. Thomas Handler, University of Tennessee, Physics Department, 404 Neilsen Physics Building, Knoxville, TN 37996
29. Harold Kirk, Brookhaven National Laboratory, P.O. Box 5000, Physics Department, Building 901A, Upton, NY 11973-5000
30. Kirk McDonald, Princeton University, Physics Department, 309 Jadwin Hall, Princeton, NJ 08544
31. Nikolai Mokhov, Fermilab, P.O. Box 500, BD-DH-Beam Physics Department, Mail Station 220, WH 12E, Batavia, IL 60510-0500
32. John R. O'Fallon, Director, High Energy Physics Division, 19901 Germantown Road, SC-22, Room G-454, Germantown, MD 20874
33. S. P. Rosen, Office of High Energy and Nuclear Physics, U.S. Department of Energy, 19901 Germantown Road, SC-20, Room H-410, Germantown, MD 20874
34. Andrew Sessler, Lawrence Berkeley National Laboratory, Accelerator and Fusion Research Division, 1 Cyclotron Road, Mailstop 71-259, Berkeley, CA 94720
35. Thomas E. Shannon, University of Tennessee, Mechanical and Aerospace Engineering and Engineering Science Department, 414 Dougherty Engineering Building, Knoxville, TN 37996
36. Alvin Tollestrup, Fermilab, P.O. Box 500, PPD-EPP Exp. Physics Projects, Mail Station 221, WH 13E, Batavia, IL 60510-0500
37. P. K. Williams, High Energy Physics Division, 19901 Germantown Road, SC-22, Room G-447, Germantown, MD 20874
38. Michael Witherell, Fermilab, P.O. Box 500, DO-Directorate, Mail Station 105, WE 2E, Batavia, IL 60510-0500
39. Bernhard Zeitnitz, Forschungszentrum Karlsruhe GmbH, Institut für Kernphysik I, postfach 3640, D-76021 Karlsruhe, Germany
40. Christian Zeitnitz, Institut fuer Physik, Universitaet 55099 Mainz, Germany
41. Michael Zisman, Lawrence Berkeley National Laboratory, Accelerator and Fusion Research Division, 1 Cyclotron Road, Mailstop 71-259, Berkeley, CA 94720
42. Office of Scientific and Technical Information, P.O. Box 62, Oak Ridge, TN 37831